CrystEngComm

Accepted Manuscript

This article can be cited before page numbers have been issued, to do this please use: H. Andleeb, I. Khan, A. Franconetti, M. N. Tahir, J. Simpson, S. Hameed and A. Frontera, *CrystEngComm*, 2019, DOI: 10.1039/C8CE01917G.

ROYAL SOCIETY OF CHEMISTRY

rsc.li/crystengcomm

View Article Online
DOI: 10.1039/C8CE01917G

Diverse structural assemblies of U-shaped hydrazinyl-sulfonamides: experimental and theoretical analysis of non-covalent interactions stabilizing the solid state conformations

Hina Andleeb,[a] Imtiaz Khan,[a,b] Antonio Franconetti,[c] Muhammad Nawaz Tahir,[d] Jim Simpson,[e] Shahid Hameed,[a,*] Antonio Frontera[c,*]

[a]Department of Chemistry, Quaid-i-Azam University, Islamabad-45320, Pakistan

[b]School of Chemistry & Manchester Institute of Biotechnology, The University of Manchester, 131 Princess Street, Manchester M1 7DN, United Kingdom

[c]Departament de Química, Universitat de les Illes Balears, Crta de Valldemossa km 7.5, 07122 Palma de Mallorca (Baleares), Spain

[d]Department of Physics, University of Sargodha, Sargodha, Pakistan

[e]Department of Chemistry, University of Otago, P.O. Box 56, Dunedin, 9054, New Zealand

***Corresponding authors**. E-mail: shameed@qau.edu.pk (S. Hameed); Tel.: +92-51-9064-2133; Fax: +92-51-9064-2241; E-mail: toni.frontera@uib.es (A. Frontera); Tel: +34 971 259576; Fax: +34 971 17 27 63

View Article Online
DOI: 10.1039/C8CE01917G

Abstract

The present study unfolds the synthesis of five new hydrazinyl-sulfonamide derivatives incorporating linear and branched alkyl chains. An efficient and straightforward synthetic approach was realized to achieve these sulfonamide compounds in good yields. The synthesized compounds were fully characterized by spectroscopic methods and single crystal X-ray diffraction analysis. Structural analysis of U-shaped hydrazinyl-sulfonamides reveals the presence of remarkable similarities in their crystal packing. Supramolecular architectures of these molecules were stabilized by the classical hydrogen bonds and C—H···O interactions. Furthermore, the U-shaped conformation observed in the solid state of all compounds has been analyzed using DFT calculations, AIM analysis and the NCIplot index. It reveals the existence of two intramolecular interactions, which are NH···π and unconventional π–π interactions involving the hydrazido π-system.

Introduction

Sulfonamides are the diverse structural pharmacophores prevalent in nearly 200 drugs in the market which have been developed as anti-migraine, diuretics, acetylcholinesterase and cyclooxygenase-II (COX-2)-specific anti-inflammatory medicines.[1–3] Sulfonamides have also been investigated as one of the topmost inhibitors of the metallo-enzyme carbonic anhydrase with many clinical applications as antiglaucoma agents in the form of acetazolamide (AZA) and methazolamide (MZA).[4–9] Sulfonamide drugs are widely used as HIV protease,[10,11] antitumor,[12] anticholestrolacyl transferase,[13] and glycogen phosphorylase inhibitors.[14,15]

In addition, sulfonamide derivatives find several clinical applications as anticonvulsant,[16] antibacterial, antibiotic,[17–20] and also for the therapy of other diseases.[21,22] Moreover, sulfonamides have displayed inhibitory effects against dihydropteroate synthase (DHPS),[23] preventing the

View Article Online
DOI: 10.1039/C8CE01917G

synthesis of folic acid (vitamin B9), serine protease,[24] and matrix metalloproteinase.[25] This widespread pharmacophoric potential value of sulfonamides has led to the discovery of various other therapeutic applications such as in cancer chemotherapy and hypoglycemia.[15,26]

Non-covalent interactions are heavily involved in crystal engineering and molecular recognition,[27] showing their diverse utility as a powerful tool for the construction of supramolecular architectures.[28] Among them, nonconventional C–H/X (X = O, N, S and π electrons) hydrogen bonding[29–33] has garnered immense attention due to its involvement in supramolecular structures,[34–39] biological structures,[40–44] and anion receptors.[45–49] Inter- and intra-molecular hydrogen bonding has extensively been employed in the generation of complex organized systems due to the reversibility, specificity, directionality and cooperativity of such interactions.[50] Among the weak hydrogen bonds, C–H···π interactions are of imperative significance holding several unique features including chiral recognition, polymer chemistry, coordination chemistry, biochemistry, and the structures of DNA and proteins.[51] In view of these significant applications, it is of much interest to explore the role of non-covalent interactions in new classes of compounds forming supramolecular architectures.

In this manuscript, we report the synthesis and X-ray characterization of five new hydrazinyl-sulfonamides and a detailed description of their crystal packing and supramolecular forces responsible of their crystal growth. Moreover, we have analyzed using DFT methods and several computational tools the U-shape conformation that these molecules present in the solid state. It is governed by the formation of two simultaneous intramolecular π-interactions, which occur at the same face of the aromatic ring where the whole hydrazinyl group is involved.

Experimental

Chemicals and instrumentation

View Article Online
DOI: 10.1039/C8CE01917G

Unless otherwise noted, all commercially available reagents were used as received. All reactions were carried out using oven-dried glassware. All the reactions were monitored using pre-coated silica gel ($60F_{254}$ 0.2 mm) TLC plates from Merck (Germany). Product spots were visualized under UV light at 254 nm. Melting points were recorded on a Gallenkamp melting point apparatus (MP-D) in open capillaries and are uncorrected. Infra-red (IR) spectra were recorded on Schimadzu Fourier Transform Infra-Red Spectrophotometer model 270 using ATR (Attenuated total reflectance) facility. NMR spectra were recorded on Bruker DQX400 and AV300 spectrometers at room temperature. ^{1}H and ^{13}C NMR spectra were referenced to external tetramethylsilane *via* the residual protonated solvent (^{1}H) or the solvent itself (^{13}C). Chemical shifts (δ) are quoted in parts per million (ppm). For DMSO-d_6, the shifts are referenced to 2.50 ppm for ^{1}H NMR spectroscopy and 39.52 ppm for ^{13}C NMR spectroscopy. Coupling constant (J) values are reported to the nearest 0.5 Hz. The elemental analysis was performed on Leco CHNS-932 Elemental Analyzer, Leco Corporation (USA).

Synthesis

Preparation of *N*-arylsulfonylated amino acids (3a–e)

The corresponding amino acid (1.00 mmol) was dissolved in an aqueous solution of sodium carbonate (2.5 mmol in water (5 mL)) and a solution of arylsulfonyl chloride (1.20 mmol) in toluene (7 mL) was added. The reaction mixture was stirred vigorously at room temperature and monitored by TLC. After the completion of reaction (24 h), the organic layer was separated, and the aqueous layer was acidified with dilute hydrochloric acid. The precipitated solid was filtered and recrystallized from 80% EtOH/H_2O. The spectro-analytical data was consistent with those observed in literature.[52]

View Article Online
DOI: 10.1039/C8CE01917G

Preparation of *N*-arylsulfonylated amino esters (4a–e)

To a stirred solution of corresponding carboxylic acid **3a–c** (0.02 mol) in ethanol (30 mL) was added concentrated sulfuric acid (0.5 mL), and the reaction mixture was heated to reflux. The reaction progress was monitored by TLC at regular intervals. After completion of the reaction (4 h), the mixture was concentrated *in vacuo*. The crude solid was dissolved in ethyl acetate and washed with a 10% aqueous sodium bicarbonate (2 × 25 mL). The organic layer was dried (Na_2SO_4), filtered and concentrated *in vacuo*. The product obtained was recrystallized from 80% EtOH/H_2O.[53,54] The spectro-analytical data for **4a–d** was consistent with those observed in literature.[55]

Ethyl ((4-chlorophenyl)sulfonyl)valinate (4e)

White crystalline solid (75%): m.p 157–158 °C; R_f: 0.85 (30% ethyl acetate/*n*-hexane); IR (ATR, cm^{-1}): 3298 (NH), 1730 (C=O), 1371, 1149 (O=S=O); ^{1}H NMR (400 MHz, DMSO-d_6): δ 7.94 (1H, s, $NHSO_2$), 7.77–7.70 (2H, m, ArH), 7.64–6.59 (2H, m, ArH), 4.53 (2H, q, J = 6.9 Hz, CH_2), 3.36 (1H, s, CHC=O), 1.94–1.71 (1H, m, CH), 1.27 (3H, t, J = 6.9 Hz, CH_3), 0.78 (3H, d, J = 6.7 Hz, CH_3), 0.75 (3H, d, J = 6.7 Hz, CH_3); ^{13}C NMR (100.6 MHz, DMSO-d_6): δ 180.11 (C=O), 166.73 (C), 140.92 (C), 128.90 (2 × CH), 128.39 (2 × CH), 60.73 (CH), 42.96 (CH_2), 30.67 (CH), 18.94 (CH_3), 18.64 (CH_3), 21.40 (CH_3); Anal. calcd. for $C_{13}H_{18}ClNO_4S$ (319.06): C, 48.83; H, 5.67; N, 4.38; S, 10.03%. found: C, 48.64; H, 5.55; N, 4.23; S, 9.91%.

Preparation of hydrazinyl-sulfonamides (5a–e)

To a stirred solution of corresponding ester **4a–e** (0.01 mol) in methanol (30 mL) was added hydrazine hydrate (80%, 0.04 mol). The resulting mixture was heated at reflux and progress was monitored by TLC at regular intervals. After completion of the reaction (6 h), the mixture was

View Article Online
DOI: 10.1039/C8CE01917G

concentrated *in vacuo*. The crude solid was washed with cold water, filtered, and recrystallized from 80% EtOH/H_2O.[53,54] Compound **5d** was reported in literature,[54d] however, partial spectroscopic data have been provided.

***N*-(1-hydrazinyl-3-methyl-1-oxobutan-2-yl)-4-methylbenzene-sulfonamide (5a)**

White crystalline solid (84%): m.p 186–187 °C; R_f: 0.35 (40% ethyl acetate/*n*-hexane); IR (ATR, cm^{-1}): 3335, 3329 (NH_2), 3277 (NH), 1685 (C=O), 1326, 1156 (O=S=O); ^{1}H NMR (400 MHz, DMSO-d_6): δ 8.98 (1H, s, NHC=O), 7.75 (1H, d, J = 8.3 Hz, $NHSO_2$), 7.62 (2H, d, J = 8.2 Hz, ArH), 7.34 (2H, d, J = 8.2 Hz, ArH), 3.93 (2H, br s, NH_2), 3.38-3.31 (1H, m, CHC=O), 2.36 (3H, s, $ArCH_3$), 1.81–1.67 (1H, m, $CH(CH_3)_2$), 0.77 (3H, d, J = 6.6 Hz, CH_3), 0.67 (3H, d, J = 6.6 Hz, CH_3); ^{13}C NMR (100.6 MHz, DMSO-d_6): δ 169.43 (C=O), 142.24 (C), 138.51 (C), 129.15 (2 × CH), 126.51 (2 × CH), 60.64 (CH), 30.68 (CH_3), 20.99 (CH), 18.94 (CH_3), 18.58 (CH_3); Anal. calcd. for $C_{13}H_{21}N_3O_3S$ (299.13): C, 52.15; H, 7.07; N, 14.04; S, 10.71%. found: C, 52.01; H, 6.90; N, 13.82; S, 10.56%.

***N*-(1-hydrazinyl-4-methyl-1-oxopentan-2-yl)-4-methylbenzene-sulfonamide (5b)**

White crystalline solid (81%): m.p 143–145 °C; R_f: 0.39 (40% ethyl acetate/*n*-hexane); IR (ATR, cm^{-1}): 3350, 3322 (NH_2), 3044 (NH), 1687 (C=O), 1329, 1152 (O=S=O); ^{1}H NMR (400 MHz, DMSO-d_6): δ 9.11 (1H, s, NHC=O), 7.84 (1H, br s, $NHSO_2$), 7.64 (2H, d, J = 8.0 Hz, ArH), 7.34 (2H, d, J = 8.0 Hz, ArH), 3.96 (2H, br s, NH_2), 3.61 (1H, t, J = 6.9 Hz, CHC=O), 2.36 (3H, s, $ArCH_3$), 1.48–1.33 (1H, m, $CH(CH_3)_2$), 1.32–1.16 (2H, m, CH_2CHNH), 0.75 (3H, d, J = 6.6 Hz, CH_3), 0.65 (3H, d, J = 6.6 Hz, CH_3); ^{13}C NMR (100.6 MHz, DMSO-d_6): δ 170.16 (C=O), 142.35 (C), 138.40 (C), 129.21 (2 × CH), 126.54 (2 × CH), 53.25 (CH), 41.65 (CH_2), 23.78 (CH), 22.52 (CH_3), 21.72 (CH_3), 21.00 (CH_3); Anal. calcd. for $C_{12}H_{19}N_3O_3S$ (285.11): C, 50.51; H, 6.71; N, 14.73; S, 11.23%. found: C, 50.34; H, 6.52; N, 14.57; S, 11.02%.

View Article Online
DOI: 10.1039/C8CE01917G

_N_-(1-hydrazinyl-3-methyl-1-oxobutan-2-yl)-4-methoxybenzene-sulfonamide (5c)

White crystalline solid (79%): m.p 160–162 °C; R_f: 0.32 (40% ethyl acetate/*n*-hexane); IR (ATR, cm^{-1}): 3350, 3301 (NH_2), 3019 (NH), 1664 (C=O), 1328, 1149 (O=S=O); ^{1}H NMR (400 MHz, DMSO-d_6): δ 8.98 (1H, s, NHC=O), 7.73–7.58 (3H, m, $NHSO_2$ & ArH), 7.07–7.00 (2H, m, ArH), 3.96 (2H, br s, NH_2), 3.81 (3H, s, OCH_3), 3.32 (1H, br s, CHC=O), 1.80–1.65 (1H, m, $CH(CH_3)_2$), 0.75 (3H, d, J = 6.8 Hz, CH_3), 0.72 (3H, d, J = 6.8 Hz, CH_3); ^{13}C NMR (100.6 MHz, DMSO-d_6): δ 169.50 (C=O), 161.90 (C), 133.08 (C), 128.63 (2 × CH), 113.85 (2 × CH), 60.62 (OCH_3), 55.60 (CH), 30.67 (CH), 18.96 (CH_3), 18.59 (CH_3); Anal. calcd. for $C_{12}H_{19}N_3O_4S$ (301.11): C, 47.83; H, 6.36; N, 13.94; S, 10.64%. found: C, 47.64; H, 6.21; N, 13.76; S, 10.40%.

4-Chloro-_N_-(1-hydrazinyl-1-oxopropan-2-yl)benzenesulfonamide (5d)

White crystalline solid (81%): m.p 163–165 °C; R_f: 0.37 (40% ethyl acetate/*n*-hexane); IR (ATR, cm^{-1}): 3349, 3338 (NH_2), 3049 (NH), 1688 (C=O), 1330, 1152 (O=S=O); ^{1}H NMR (300 MHz, DMSO-d_6): δ 9.10 (1H, s, NHC=O), 8.16 (1H, s, $NHSO_2$), 7.79–7.75 (2H, m, ArH), 7.67–7.63 (2H, m, ArH), 4.08 (2H, br s, NH_2), 3.74 (1H, q, J = 6.6 Hz, CHC=O), 1.03 (3H, d, J = 6.9 Hz, CH_3); ^{13}C NMR (75 MHz, DMSO-d_6): δ 170.84 (C=O), 140.09 (C), 137.84 (C), 129.56 (2 × CH), 128.87 (2 × CH), 51.00 (CH), 19.25 (CH_3); Anal. calcd. for $C_9H_{12}ClN_3O_3S$ (277.03): C, 38.92; H, 4.36; N, 15.13; S, 11.54%. found: C, 38.69; H, 4.19; N, 15.00; S, 11.31%.

4-Chloro-_N_-(1-hydrazinyl-3-methyl-1-oxobutan-2-yl)benzenesulfonamide (5e)

White crystalline solid (87%): m.p 181–183 °C; R_f: 0.35 (40% ethyl acetate/*n*-hexane); IR (ATR, cm^{-1}): 3367, 3330 (NH_2), 3298 (NH), 1687 (C=O), 1373, 1153 (O=S=O); ^{1}H NMR (400 MHz, DMSO-d_6): δ 9.05 (1H, s, NHC=O), 7.95 (1H, br s, $NHSO_2$), 7.76–7.69 (2H, m, ArH), 7.65–6.58 (2H, m, ArH), 3.98 (2H, br s, NH_2), 3.37 (1H, br s, CHC=O), 1.82–1.66 (1H, m, $CH(CH_3)_2$, 0.77 (3H, d, J = 6.7 Hz, CH_3), 0.74 (3H, d, J = 6.7 Hz, CH_3); ^{13}C NMR (100.6 MHz, DMSO-d_6): δ

View Article Online
DOI: 10.1039/C8CE01917G

169.11 (C=O), 140.23 (C), 136.92 (C), 128.90 (2 × CH), 128.39 (2 × CH), 60.73 (CH), 30.67 (CH), 18.94 (CH_3), 18.64 (CH_3); Anal. calcd. for $C_{11}H_{16}ClN_3O_3S$ (305.06): C, 43.21; H, 5.27; N, 13.74; S, 10.48%. found: C, 43.04; H, 5.05; N, 13.53; S, 10.29%.

Crystal growth development

Single crystals of compounds **5a–e** suitable for X-ray diffraction analysis were grown at room temperature from ethanol solvent.

X-ray structure determination

Crystallographic data for compounds **5a**–**e** are listed in Table 1. Diffraction data were collected on a Bruker APEXII CCD diffractometer using graphite-monochromated Mo-Kα radiation (λ = 0.71073 Å). Data collections were controlled by *APEX2* software[56] with cell refinement and data reduction performed using *SAINT*.[56] Multi-scan absorption corrections were applied using *SADABS*.[56] The structures were all solved with *SHELXS*[57] and refined by full-matrix least-squares on F^2 using *SHELXL-2014/7*.[58] All non-hydrogen atoms were assigned anisotropic displacement parameters. The H atoms on the three N atoms in each molecule were located in difference Fourier maps and their coordinates refined with their atomic displacement parameters set to $1.2U_{eq}$(N). All other H-atoms were positioned geometrically and refined using a riding model with d(C-H) = 0.93 Å for aromatic and 0.98 Å for CH with $U_{iso} = 1.2U_{eq}$(C) and 0.96 Å, $U_{iso} = 1.5U_{eq}$(C) for CH_3 atoms. All molecular plots and packing diagrams were drawn using *Mercury*.[59] Other calculations were performed using *PLATON*[60] and tabular material was produced using *WINGX*.[61]

Theoretical Methods

The geometries were fully optimized using the M06-2X/def2-TZVP level of theory by means of the G09 program package.[62] The Bader's quantum theory of "atoms-in-molecules" analysis (QTAIM) has been performed at the same level of theory, using the AIMAll program.[63] The NCI plot is a visualization index based on the electron density and its derivatives, and enables

View Article Online
DOI: 10.1039/C8CE01917G

identification and visualization of non-covalent interactions efficiently. The isosurfaces correspond to both favorable and unfavorable interactions, as differentiated by the sign of the second density Hessian eigenvalue and defined by the isosurface color. NCI analysis allows an assessment of host–guest complementarity and the extent to which weak interactions stabilize a complex. The information provided by NCI plots is essentially qualitative, i.e. which molecular regions interact. The color scheme is a red-yellow-green-blue scale with red for ρ_{cut}^{+} (repulsive) and blue for ρ_{cut}^{-} (attractive). Yellow and green surfaces correspond to weak repulsive and weak attractive interactions, respectively.[64]

Table 1 Crystal data and structure refinement of **5a–e**

	5a	**5b**	**5c**	**5d**	**5e**
Empirical formula	$C_{12}H_{19}N_3O_3S$	$C_{13}H_{21}N_3O_3S$	$C_{12}H_{19}N_3O_4S$	$C_9H_{12}ClN_3O_3S$	$C_{11}H_{16}ClN_3O_3S$
Formula weight	285.36	299.39	301.36	277.73	305.78
Temperature (K)	296(2)	296(2)	296(2)	296(2)	296(2)
Wavelength (Å)	0.71073	0.71073	0.71073	0.71073	0.71073
Crystal system	Monoclinic	Monoclinic	Monoclinic	Monoclinic	Monoclinic
Space group	P 21	P 21	P 21	P 21	P 21
a (Å)	7.6720(11)	10.3216(9)	10.4333(7)	10.0850(5)	10.4296(6)
b (Å)	9.7977(13)	6.6441(5)	6.8279(4)	6.6661(3)	6.7642(3)
c (Å)	9.9187(13)	12.0540(11)	11.1774(7)	18.9899(9)	11.2829(6)
α (°)	90	90	90	90	90
β (°)	90.011(5)	105.426(4)	113.332(4)	104.813(3)	113.623(3)
γ (°)	90	90	90	90	90
V (A^3)	745.57(18)	796.86(12)	731.14(8)	1234.22(10)	729.28(7)
Z	2	2	2	4	2
D_{calc} (g cm^{-3})	1.271	1.248	1.369	1.495	1.392
μ (mm^{-1})	0.225	0.214	0.238	0.479	0.412
F (000)	304	320	320	576	320
Crystal size (mm)	0.42 × 0.28 × 0.25	0.42 × 0.34 × 0.32	0.38 × 0.30 × 0.26	0.36 × 0.24 × 0.20	0.40 × 0.22 × 0.18
Theta range for data collection	2.053 to 27.364	1.753 to 27.120	1.984 to 27.267	1.109 to 27.460	2.249 to 27.862
Reflections collected independent observed	6038 3186 [R(int) = 0.0317] 2857	6854 2788 [R(int) = 0.0184] 2608	6469 3061 2731	10868 5580 [R(int) = 0.0237] 5007	6483 3285 [R(int) = 0.0220] 2892
Min. and max. transmission	0.948 and 0.912	0.936 and 0.915	0.942 and 0.914	0.911 and 0.848	0.932 and 0.851
Data/restraints/parameters	3186 / 1 / 189	2788 / 1 / 196	3061 / 1 / 196	5580 / 1 / 333	3285 / 1 / 186
Goodness-of-fit	1.056	1.039	1.032	1.054	1.059
Final R indices [I >2σ(I)]	R_1 = 0.0349, wR_2 = 0.0928	R_1 = 0.0309, wR_2 = 0.0801	R_1 = 0.0332, wR_2 = 0.0748	R_1 = 0.0355, wR_2 = 0.0883	R_1 = 0.0357, wR_2 = 0.0947
R indices (all data)	R_1 = 0.0402, wR_2 = 0.0965	R_1 = 0.0339, wR_2 = 0.0824	R_1 = 0.0394, wR_2 = 0.0784	R_1 = 0.0410, wR_2 = 0.0920	R_1 = 0.0419, wR_2 = 0.1003

View Article Online
DOI: 10.1039/C8CE01917G

Largest difference peak and hole (e Å^{-3})	0.198 and -0.224	0.148 and -0.263	0.189 and -0.198	0.167 and -0.274	0.191 and -0.215
CCDC reference number	1826226	1826227	1826228	1826229	1826230

Results and discussion

Synthesis

The *N*-aryl sulfonamides (**5a**–**e**) were prepared from the corresponding amino acids (**1a–c**) in three steps as depicted in Scheme 1. The amino acids were reacted with sulfonyl chlorides to afford the corresponding *N*-sulfonyl-amino acid derivatives (**3a**–**e**)[65] which on acid-catalyzed esterification with ethanol yielded the *N*-sulfonyl-amino esters (**4a**–**e**).[53,54] The hydrazination[53,54] of the **4a**–**e** using hydrazine hydrate (80%) in methanol furnished the desired hydrazinyl-sulfonamides (**5a**–**e**) in good yields (79–87%).

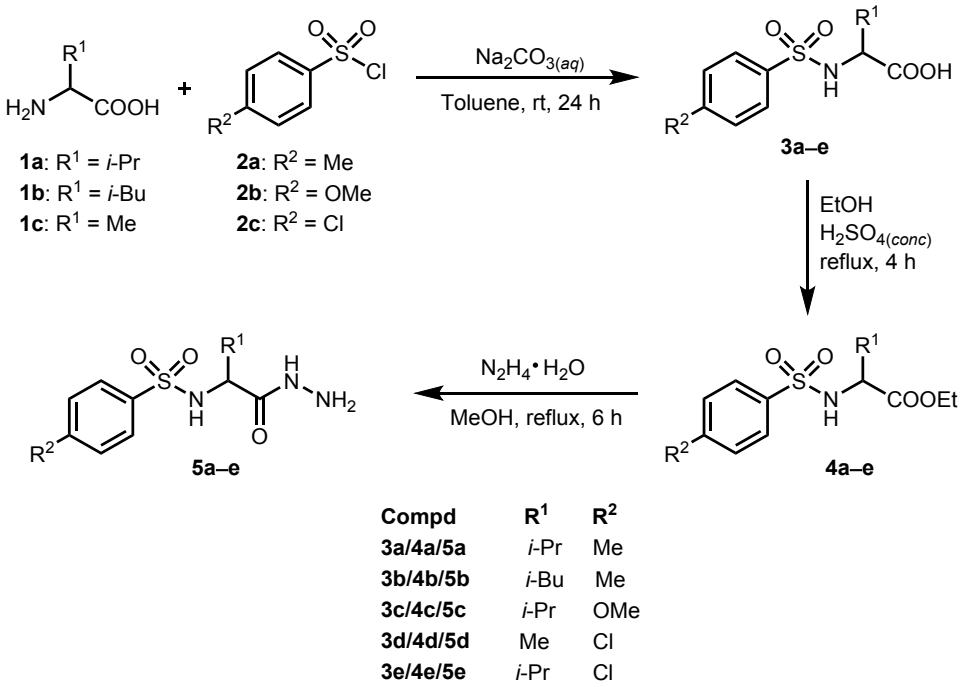

Scheme 1 Synthesis of hydrazinyl-sulfonamides (**5a–e**).

X-ray crystallography

Structural background

View Article Online
DOI: 10.1039/C8CE01917G

A search of the Cambridge structural database (Version 5.37 Nov. 2015 with 2 updates) reveals the structural novelty of the compounds reported here with no 1-hydrazinylbenzenesulfonamide reported previously. Indeed, the two reported structures, closest in to those reported here, are (*E*)-4-methyl-*N*-(2-(2-(4-methylbenzylidene)hydrazino)-2-oxoethyl)benzenesulfonamide[66] and (*E*)-*N*-(2-(2-(3-chlorobenzylidene)hydrazinyl)-2-oxoethyl)-4-methylbenzenesulfonamide monohydrate.[67] Clearly the scarcity of structures reflects the presence of the hydrazinyl portion of the molecule as a search for structures containing the C-C(O)-NH-NH_2 fragment produced no hits. In stark contrast, 2194 hits were recorded in a search for the $C_6H_4SO_2NHC$ fragment allowing for substitution at the 4-position of the benzene ring.

Molecular structures

Single crystals of compounds **5a–e** (Scheme 1) were grown at room temperature from ethanol solvent and their molecular structures are shown in Fig. 1(a–e). Bond lengths and angles are given in Tables S1–S10 (ESI).

View Article Online
DOI: 10.1039/C8CE01917G

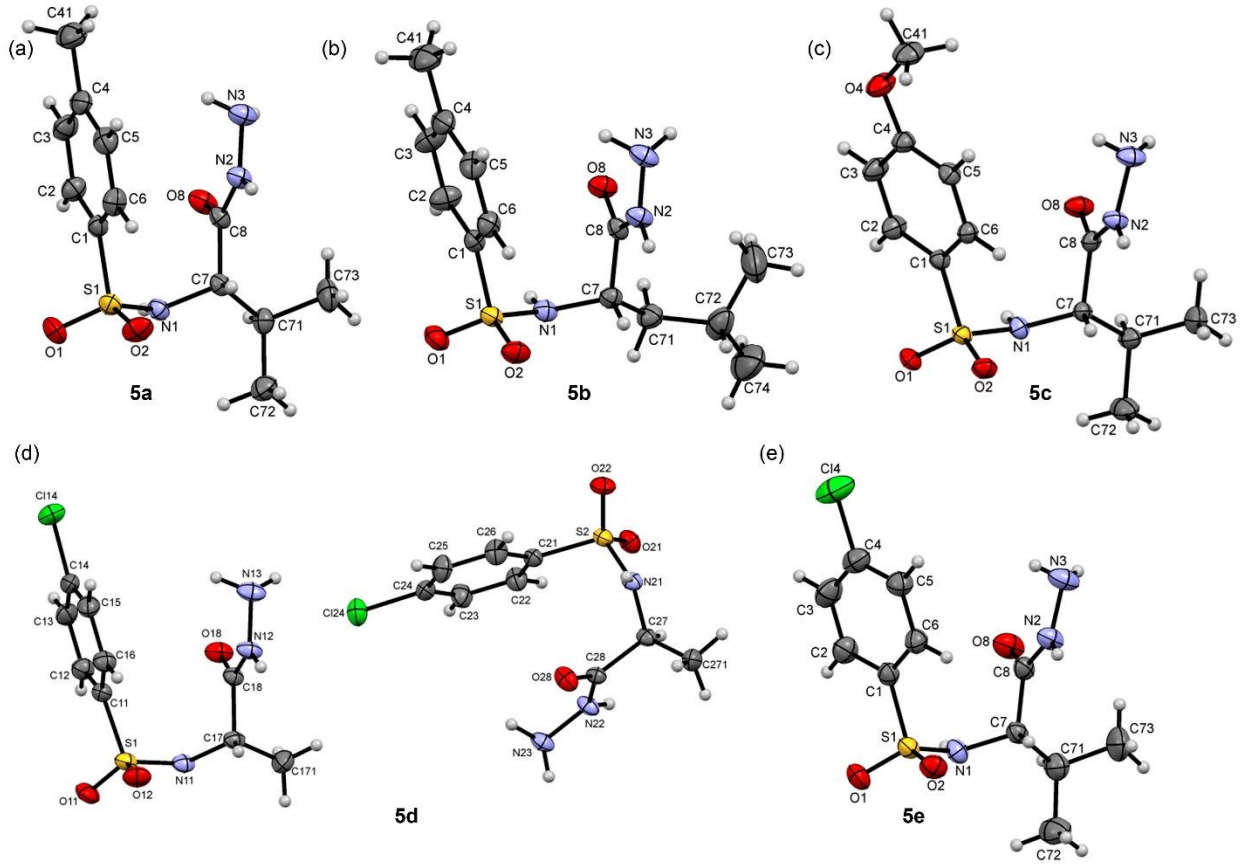

Fig. 1 The molecular structures of (a) **5a**, (b) **5b**, (c) **5c** and (d) the asymmetric unit of **5d** and (e) **5e** showing the atom numbering with ellipsoids drawn at the 50% probability level.

The molecular structures of **5a–c** and **5e** are sufficiently similar to be discussed together. All four molecules are U shaped, Fig. 1 (a–c, e), with sulfonamide N1 atoms at the base of each U and the *i*-propyl substituents of **5a** and **5c** and the *i*-butyl substituent of **5b** on the C7 atoms pointing away from the us. The benzene rings each carry sulfonamide substituents at C1 bound through the S1 atoms with each ring also substituted in the 4-position with methyl groups for **5a** and **5b** and a methoxy substituent in **5d**. The planes of the benzene rings are each inclined to the corresponding hydrazide planes by 17.20(10)° for **5a**, 19.28(15)° for **5b** and 36.09(9)° for **5c**. Compound **5d** crystallizes with two unique molecules, 1 and 2, in the asymmetric unit, Fig 1(d) with both molecules showing striking similarities to those of **5a–c**. The unique molecules are differentiated

View Article Online
DOI: 10.1039/C8CE01917G

by leading 1 and 2 characters in the atom numbering. As with **5a–c**, both molecules are U shaped, Fig. 1, with sulfonamide N11 and N21 atoms at the base of each U and the methyl substituents on C17 and C27 pointing away from the us. The two molecules overlay (Mercury) with an rms deviation of 0.112 Å with minor differences between the conformations of the C171 and C271 methyl substituents and the O18 and O28 carbonyl O atoms, Fig. 2. This variation is also reflected in the relative inclinations of the benzene and hydrazide mean planes as the planes of the 4-chloro substituted benzene rings are inclined to the planes of the hydrazide units by 16.9(2)° and 21.9(2)° for molecules 1 and 2 respectively. Compound **5e** also retains the characteristic U shape again with a chloro-substituent on the 4-position of the benzene but with an *i*-propyl group on C7. The benzene ring is inclined to the hydrazide unit at an angle of 35.01(11)°.

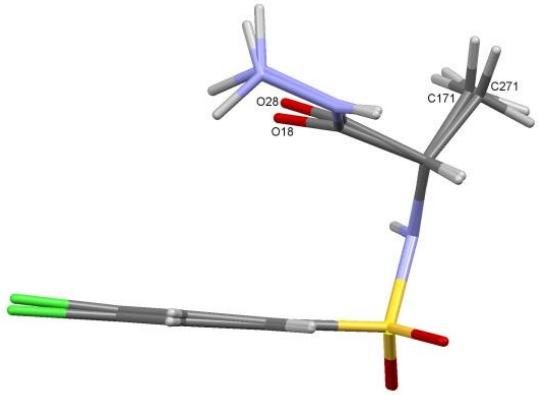

Fig. 2 An overlay (Mercury) of the two unique molecules in the asymmetric unit of **5d**.

Crystal packing

Hydrogen bond distances and angles for **5a**–**e** are given in Table 2. As with the molecular structures, the similarities in the crystal packing of the five structures, each of which crystallizes in the monoclinic space group P 21 with $Z = 2$ for **5a**–**c** and **5e** but with two unique molecules in the asymmetric unit $Z = 4$ for **5d**, are such that their crystal packing can be discussed together. A striking commonality in the packing of all five molecules is that the N-H groups of the sulfonamide

View Article Online
DOI: 10.1039/C8CE01917G

and hydrazinyl groups of the molecules are all involved in classical N-H…N and N-H…O hydrogen bonds, Table 2. The sulfonamide N1, N11 and N12 atoms invariably act as strong N-H…N hydrogen bond donors while the N2, N3, N12, N13, N22 and N23 atoms of the hydrazinyl groups form N—H…O hydrogen bonds for **5a**–**c** and **5e** but a more eclectic mix of N—H…O and N—H…Cl contacts for **5d**.

Another common feature of the packing for all five molecules is the formation of sheets of molecules parallel to one of the crystallographic axes as shown in Figs. 3-7. For **5a-c** these are generated by N—H…O (N…O distances in the range 2.826(3) to 3.188(3) Å), N—H…N (N…N distances in the range 2.907(3) to 2.972(4) Å), and much weaker C—H…O hydrogen bonds (C…O distances in the range 3.216(4) to 3.601(3) Å), Table 2.

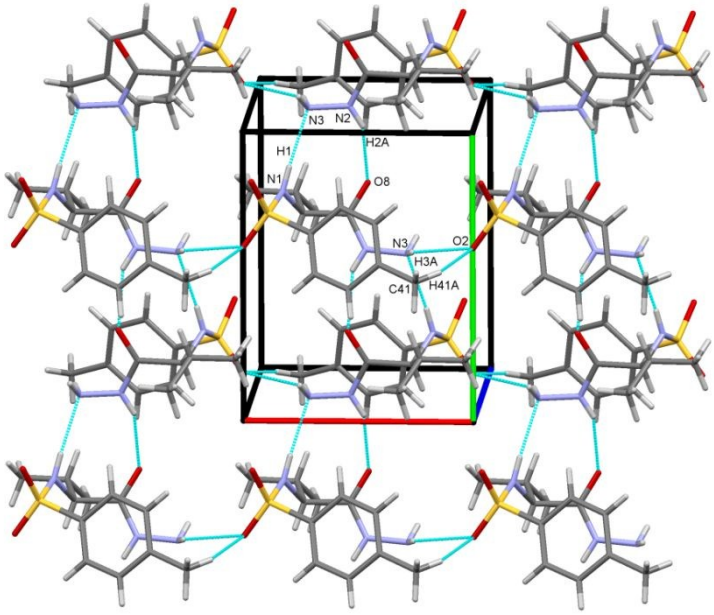

Fig. 3 Sheets of molecules of **5a** along the *b* axis.

View Article Online
DOI: 10.1039/C8CE01917G

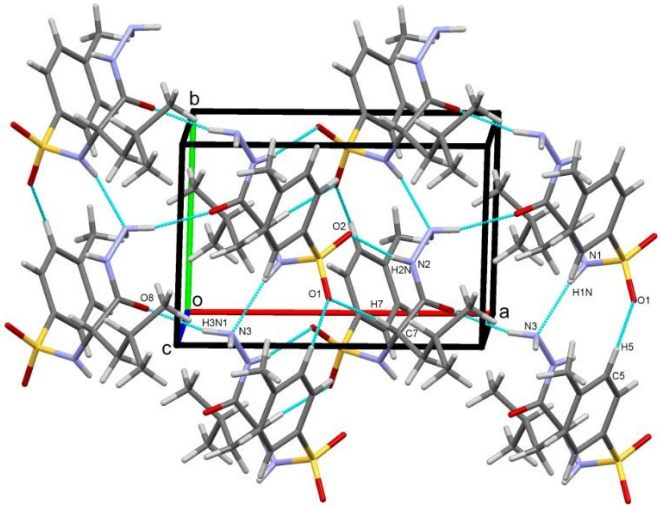

Fig. 4. Sheets of molecules of **5b** in the *ab* plane.

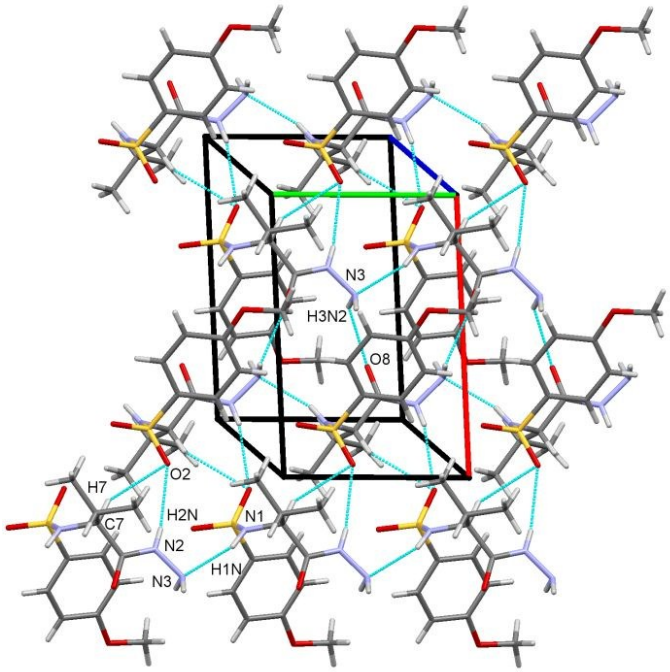

Fig. 5 Sheets of molecules of **5c** in the *ab* plane.

In **5d**, the presence of chloro-substituents on the benzene rings of the two unique molecules offer additional hydrogen bonding opportunities. Despite this however, strong similarities are again

View Article Online
DOI: 10.1039/C8CE01917G

observed with the packing described previously for the analogous systems. Classical N—H···O (N…O distances in the range 2.997(4) to 3.118(5) Å), and N—H···N hydrogen bonds (N…N distances 2.905(4) and 2.925(4) Å), are augmented by a single N23—H23···Cl14 hydrogen bond (N23…Cl14 = 3.859(4) Å, Table 2. The complex packing in this system again results in sheets of molecules forming in the *bc* plane, Fig. 6, as a result of additional weak C—H…O contacts (C…O = 3.504(4) and 3.148(5) Å) and a single C171—H172…Cl14 hydrogen bond (C1712…Cl14 = 3.886(5) Å.

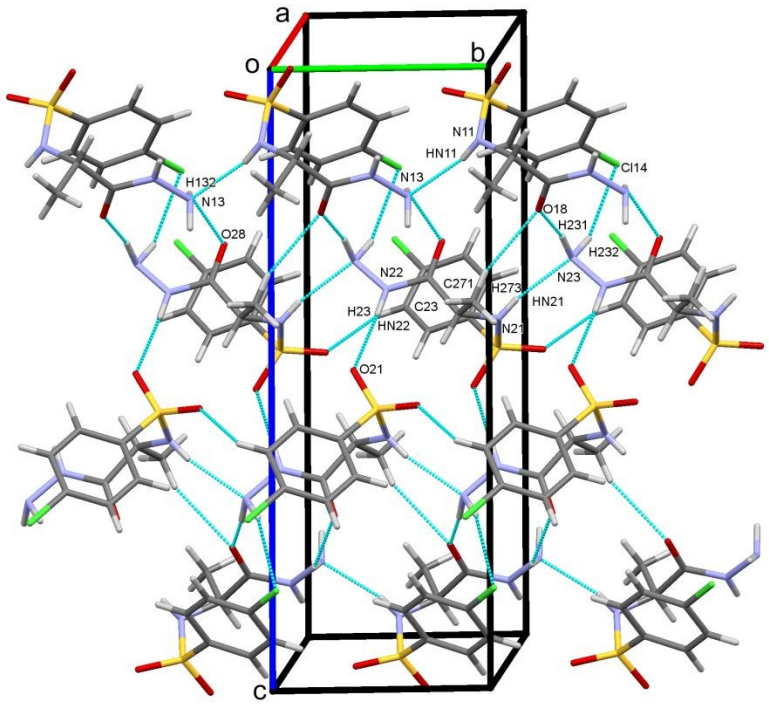

Fig. 6. Sheets formed in the *bc* plane by the two unique molecules of **5d**.

Unlike the situation for **5d**, the presence of the chloro-substituent on the aromatic ring of **5e** has a lesser impact on the crystal packing with no N—H···Cl or C—H···Cl contacts observed. Nonetheless, the ubiquitous formation of sheets of molecules is again found in the N1—H1N···N3 (N1···N3 = 2.893(4) Å), and N—H···O hydrogen bonds (N…O 2.164(3) and 2.868(4) Å) that

View Article Online
DOI: 10.1039/C8CE01917G

together with a C—H···O contact (C5…O1 = 3.230(4) Å) build sheets of molecules in the *ab* plane, Fig. 7. An unusual feature of the packing for **5e** is the observation of a weak and unusual C4—Cl4---Cg1^{i} contacts (Cg1 is the centroid of the C1···C6 benzene ring; i = -X,-1/2+Y,-Z) with the Cl···Cg1 distance 3.763(2) Å, contacts that link adjacent sheets to generate a three dimensional network, Fig. 8.

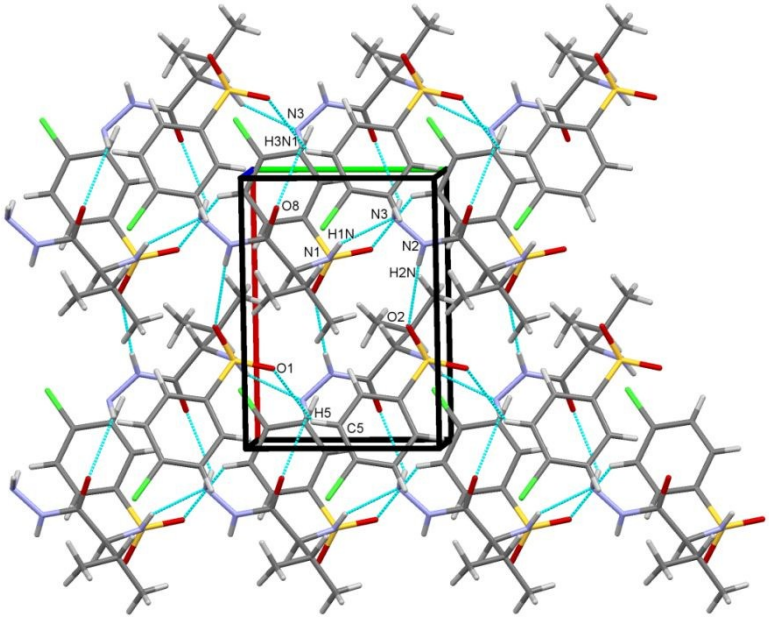

Fig. 7. Sheets of molecules of **5e** in the *ab* plane.

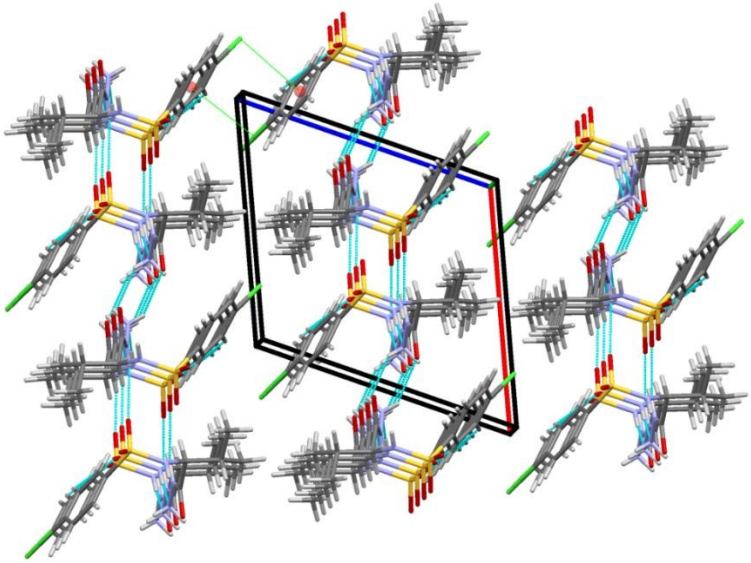

View Article Online
DOI: 10.1039/C8CE01917G

Fig. 8. Overall packing for **5e** viewed along the *b* axis direction. Representative C—Cl···π contacts are drawn as green dotted lines with the ring centroids shown as red spheres.

Stacking of the sheets formed by the other structures **5a-d** is another common feature of the packing of these compounds. Fig. 9 shows the stacks formed in the overall packing of **5a** as a representative example with the stacks formed by **5b-d** available in the supplementary material (Figs. S1-3).

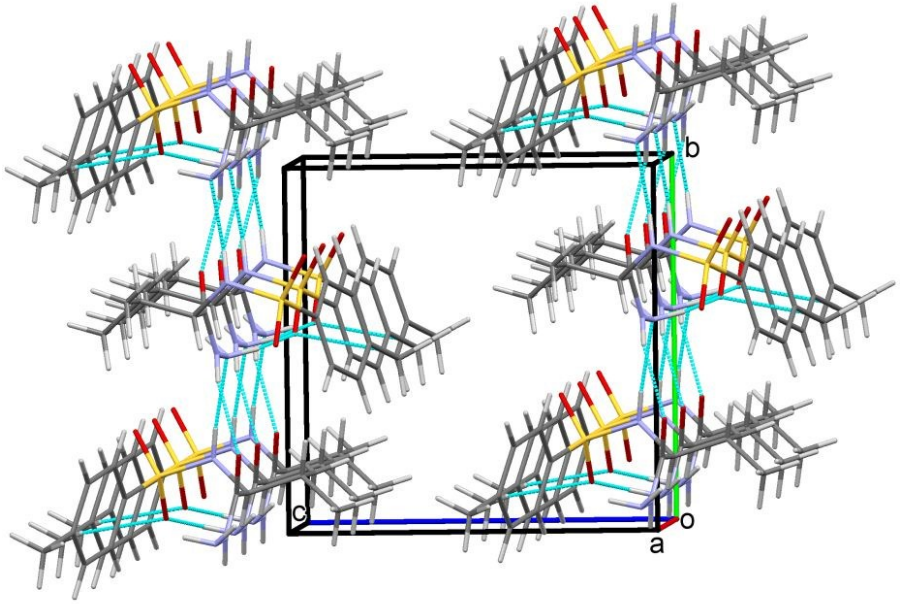

Fig. 9 Overall packing for **5a** viewed along the *a* axis direction

View Article Online
DOI: 10.1039/C8CE01917G

Table 2 Hydrogen bond distances (Å), angles (°) for **5a–e**

Compound	D—H···A	D—H	H···A	D···A	‹ D—H···A
5a	N1-H1...N3^{1i}	0.79(4)	2.13(4)	2.925(4)	175(3)
	N2-H2A...O8^{1ii}	0.80(4)	2.11(4)	2.826(3)	150(3)
	N3-H3A...O2^{1iii}	0.83(4)	2.31(4)	2.894(4)	128(4)
	C41-H41A...O2^{1iii}	0.96	2.58	3.447(5)	151
5b	N1-H1N...N3^{2i}	0.82(3)	2.12(3)	2.907(3)	163(3)
	N2-H2N...O2^{2ii}	0.81(3)	2.22(3)	3.025(3)	169(3)
	N3-H3N1...O8^{2iii}	0.91(3)	2.08(3)	2.978(3)	167(3)
	C5-H5...O1^{2iv}	0.93	2.65	3.216(4)	120
	C7-H7...O1^{2ii}	0.98	2.65	3.580(3)	159
5c	N1-H1N...N3^{3i}	0.80(3)	2.21(3)	2.972(4)	159(3)
	N2-H2N...O2^{3ii}	0.79(3)	2.42(3)	3.188(3)	166(3)
	N3-H3N2...O8^{3iii}	0.79(3)	2.39(4)	2.967(4)	130(3)
	C7-H7...O2^{3ii}	0.98	2.72	3.601(3)	150
5d	N23-H231...O18^{4i}	0.95(4)	2.08(4)	2.997(4)	162(4)
	N23-H232...Cl14^{4i}	1.04(4)	2.86(4)	3.859(4)	161(3)
	N11-HN11...N13^{4ii}	0.77(4)	2.15(5)	2.905(4)	166(4)
	N12-HN12...O12^{4iii}	0.79(4)	2.21(4)	2.997(4)	169(4)
	N13-H132...O28^{4iv}	0.92(5)	2.51(5)	3.118(5)	123(4)
	N21-HN21...N23^{4v}	0.78(4)	2.16(4)	2.925(4)	167(4)
	N22-HN22...O21^{4vi}	0.83(4)	2.20(4)	3.006(4)	165(4)
	C17-H17...O11^{4iii}	0.99	2.68	3.504(4)	142
	C171-H172...Cl14^{4i}	0.96	2.94	3.886(5)	169
	C23-H23...O22^{4ii}	0.93	2.58	3.148(5)	119
5e	N1-H1N...N3^{5i}	0.74(4)	2.21(4)	2.893(4)	153(4)
	N2-H2N...O2^{5ii}	0.80(4)	2.37(4)	3.164(3)	169(3)
	N3-H3N1...O8^{5iii}	0.72(4)	2.36(5)	2.868(4)	129(5)
	C5-H5...O1^{5iv}	0.93	2.65	3.230(4)	121

Symmetry codes: 1i = 1 -x+1,y+1/2,-z; 1ii = -x+1,y-1/2,-z; 1iii = x+1,y,z; 2i = x,y-1,z; 2ii =-x+1,y+1/2,-z+2; 2iii = -x+2,y+1/2,-z+2; 2iv = x,y+1,z; 3i = x,y+1,z; 3ii = -x,y-1/2,-z; 3iii = -x+1,y-1/2,-z; 4i = x-1,y,z; 4ii = x,y-1,z; 4iii = -x+1,y+1/2,-z; 4iv = x+1,y,z; 4v = x,y+1,z; 4vi = -x,y-1/2,-z+1; 5i = x,y+1,z; 5ii = -x+1,y-1/2,-z+1; 5iii = -x,y-1/2,-z+1; 5iv = x,y-1,z .

Theoretical (DFT) study

As commented above in the structural description of the compounds reported herein, the supramolecular assemblies observed in their crystal structures are basically dominated by different

View Article Online
DOI: 10.1039/C8CE01917G

networks of hydrogen bonding interactions. This is basically due to the presence of two functional moieties that are rich in H-bond donor/acceptor groups, namely the hydrazido and the sulfonamide moieties. The MEP analysis is almost identical for all the structures in terms of the most nucleophilic and electrophilic parts of the molecules, and we report the results for **5d** as a typical example. We first computed the MEP surface of the M06-2X/def2-TZVP optimized geometry of compound **5d** in Fig. 10. We also calculated the molecular electrostatic potential (MEP) using this optimized geometry and plotted it onto the approximate van der Waals surface (isosurface 0.001 a.u.). This type of representation is very useful to distinguish the nucleophilic and electrophilic parts of a molecule and to rationalize the noncovalent interactions. From an inspection of the MEP surface shown in Fig. 10 it is evident that the most electron-rich region corresponds to the vicinity of the O-atoms of the sulfonamide group, which are the best H-bond acceptors. The carbonyl O-atom and the lone pair at the sp^3 hybridized N-atom of the hydrazido group are also good H-bond acceptors, as is seen in the crystal packing of the compounds. The MEP surface also indicates that the NH group of the hydrazydo group is the best H-bond donor (205 kJ/mol) followed by the NH and NH_2 groups of the sulfonamide and hydrazido moieties, respectively. The van der Waals surface also indicates a strong overlap between the hydrazido group and the π-system of the aromatic ring, which is discussed further below.

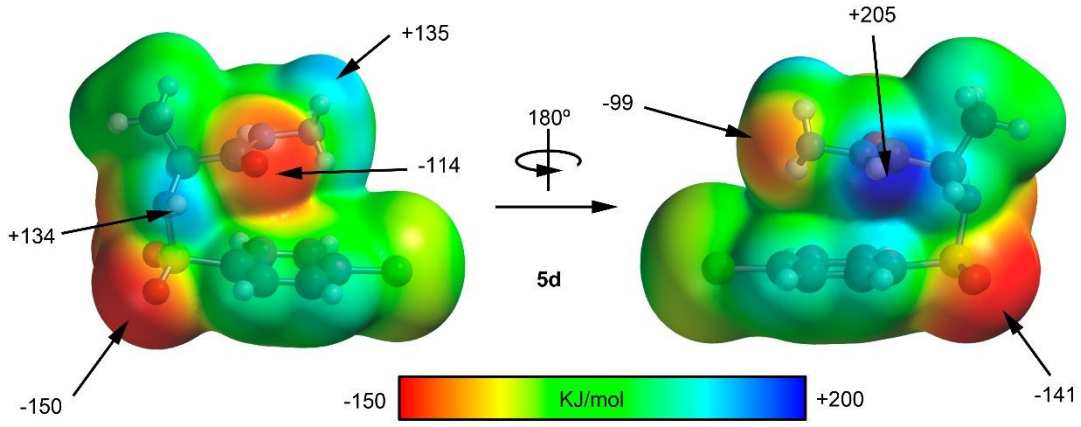

View Article Online
DOI: 10.1039/C8CE01917G

Fig. 10 MEP (two orientations) of compound **5d** plotted onto the 0.001 a.u. isodensity surface. The energies at selected points of the surfaces are given in kJ/mol.

We have used the DFT study to analyze the U-shape conformation adopted for all of the compounds reported here and to examine the π-interactions of the hydrazido groups with the benzene rings as anticipated by the examination of the van der Waals surface. Furthermore, we have also analyzed how the substituent in *para* position (chloro-, methyl- or methoxy) influences the intramolecular interactions.

In Fig. 11 we show the optimized theoretical models we have used for this study where R^1 is methyl in all cases and R^2 = Cl, Me and OMe, which are denoted as **I**, **II** and **III**, respectively. It is expected that the substitution of *i*-Pr or *i*-Bu by methyl in these theoretical models does not influence the ability of hydrazinyl-sulfonamides to adopt the U-shaped conformation. In fact, for R^2 = Me we have carried out the calculations for *i*-Pr or *i*-Bu obtaining almost identical results. For each model we have computed two conformations: U-shape (A) and a rotated one (B) where the hydrazido group is not located over the π-system (Fig. 11). A conformational search (see ESI for details) performed for R^2 = Cl and R^1 = Me (compound **5d**) indicates that the open conformation shown in Fig. 11d is the second most stable. The optimized U-shaped conformations are in all cases more stable than the rotated ones, with energy difference varying from 7.55 to 8.02 kJ/mol. A close examination of the interactions reveals two different contributions, one hand a N-H···π contact between the -NH_2 group and one C atom of the ring and also a pseudo π-stacking between the π-system of the –NHCO– unit and the aromatic ring. The relevant interatomic distances are also shown in Figure 11. While these contacts are somewhat longer than those found in a typical range of such π-interactions the QTAIM analysis discussed below clearly identifies

View Article Online
DOI: 10.1039/C8CE01917G

these weak contacts through the observation of of critical points and bond paths. Clearly therefore these contacts play a significant role in the establishment of the lower energy U-conformation of these molecules. It is also interesting to note that the NH···π interaction distances shorten as the electron donation ability of the ring substituent increases, as is common in this type of bonding. All distances are slightly shorter than the experimental ones, likely due to the absence of the neighboring molecules in the calculations.

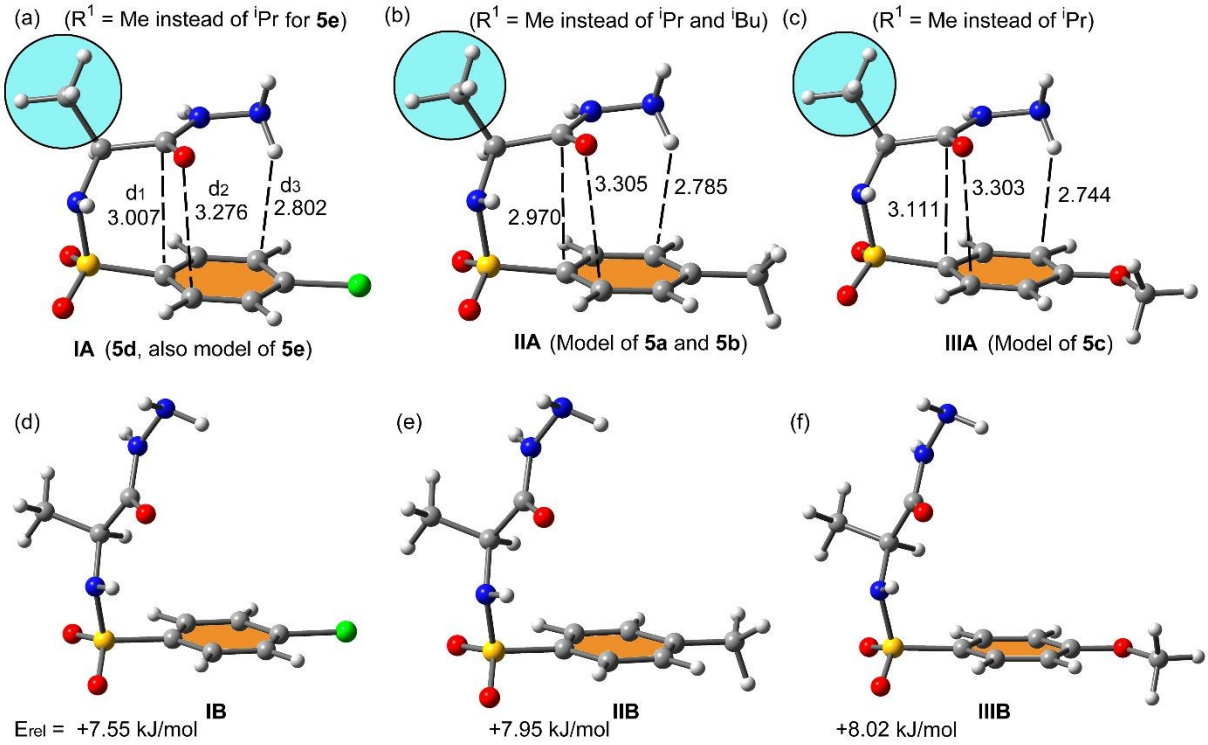

Fig. 11 M06-2x/def2-TZVP optimized geometries of models **I**, **II** and **III**, using the U-shaped (a-c, A series) and open conformations (d-f, B series). Distances in Angstroms. The relative energies are also indicated.

To further characterize the interactions discussed above that explain the U-shaped conformation of the compounds, we have used Bader's quantum theory of atoms-in-molecules (QTAIM). In Fig.

View Article Online
DOI: 10.1039/C8CE01917G

12 (top) we show the QTAIM distribution of critical points and bond paths. The presence of a bond critical point (CP) and bond path connecting two atoms is an unambiguous evidence of interaction.[68] The QTAIM analysis reveals the existence of two bond CPs and bond paths. One connects the H atom of the NH_2 group to the C atom of the benzene ring adjacent to the substituent, thus confirming the existence of the NH···π interactions in all three compounds. Close to each bond CP we also indicate the value of the density at that CP [ρ(r) in a.u.]. It is well known that the value of ρ(r) at the bond CP is an indication of the strength of the interaction.[69] It is clear that the value of ρ(r) at the bond CP that characterizes the NH···π interaction increases on going from **I** to **III**, in good agreement with the NH···C distances (Fig. 12). The other CP and bond path connects the C atom of the carbonyl to one C atom of the ring, also revealing the existence of interaction. However, neither the O atom or the N atom participate in the distribution of CPs and bond paths. At this point we have also employed the NCIplot index. The NCI plot enables the visualization and identification of non-covalent interactions efficiently, because it allows an assessment of host–guest complementarity and the extent to which such weak interactions stabilize a complex.[70] Representations of the NCI plots are shown in Fig. 12 (bottom). It can be seen that in all models a small green isosurface is present between the $–NH_2$ group and the C atom of the ring thus characterizing the NH···π interaction. In addition, a more extended isosurface is located between the π-system of the –NHCO– group and three C atoms of the aromatic ring thus confirming the existence of this unconventional π-stacking interaction. The extension and shape of the isosurface is similar in the three complexes.

View Article Online
DOI: 10.1039/C8CE01917G

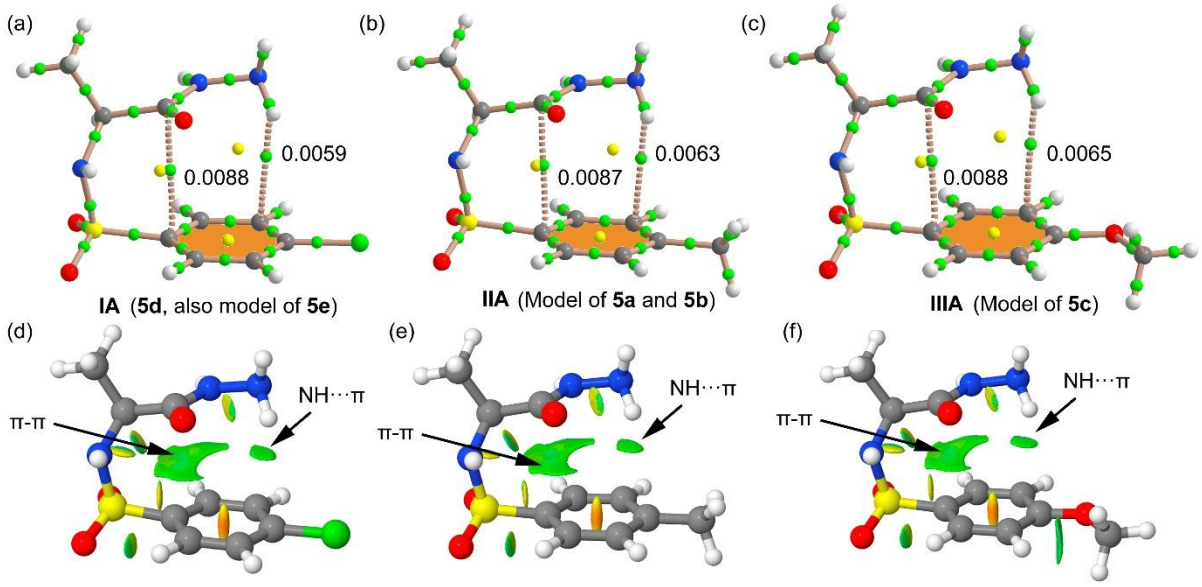

Fig. 12 (a-c) Distribution of bond (green spheres) and ring (yellow spheres) critical points in Compounds **IA-IIIA** The bond paths are also indicated (dashed lines for noncovalent interactions). (d-f) NCI plots compounds **IA-IIIA**. The gradient cut-off is s = 0.35 au, and the color scale is $-0.04 < \rho < 0.04$ au.

Finally, we have further analysed the importance of the N–H···π interaction for the formation of the U-shaped conformation and investigated if the unconventional π-stacking interaction itself is enough to bend the structure. To do so, we have used a model of **5a** (denoted as **IV**) where we have changed the hydrazido by an amido group. The results are summarized in Fig. 13. It can be observed that using this new model the U-shaped conformation is only +3.2 kJ/mol more favored than the open one (**IVB**) because the N–H···π is not present. This small difference can be thus attributed to the contribution of the π-stacking interaction between the π-system of the –NHCO– group, as confirmed by the existence of a green isosurface in the NCIplot (see Fig 13c) than embraces the amido group. Moreover the π-stacking distances are comparable to those observed in model **IA** (see Fig. 11a)

View Article Online
DOI: 10.1039/C8CE01917G

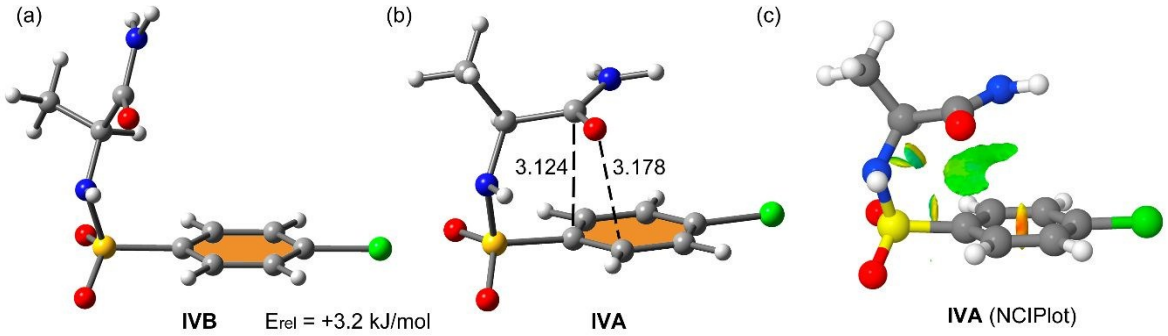

Fig. 13 M06-2x/def2-TZVP optimized geometries of model **IV**, using the open conformation (a) and U-shaped, distances in Å. (c) NCI plot of compound **IVA**. The gradient cut-off is s = 0.35 au, and the color scale is $-0.04 < \rho < 0.04$ au.

Conclusions

Five new hydrazinyl-sulfonamides (**5a–e**) with pendant linear and branched alkyl chains were efficiently synthesized in good yields. The synthesized compounds were fully characterized by spectroscopic methods and single crystal X-ray diffraction analysis. Despite the variations in the substituents on the benzene rings in these molecules and some variation in the aliphatic substituents adjacent to the sulfonamide units, the crystal packing for all four molecules shows remarkable similarities. In each case, all three N atoms form classical hydrogen bonds and these combine with C—H···O contacts to form sheets of atoms. Individual sheets may or may not be linked but in all cases, molecules are arranged in a head to tail fashion and stacked into columns along a crystallographic axis. Finally, the U-shaped conformation observed in the solid state of all compounds has been analyzed using DFT calculations, AIM analysis and the NCIplot index. It reveals the existence of two intramolecular interactions, which are NH···π and unconventional π–π

View Article Online
DOI: 10.1039/C8CE01917G

interactions involving the hydrazido π-system. To our knowledge this type on interaction where has not been previously described in the literature.

Acknowledgements

H.A. is grateful to the Higher Education Commission of Pakistan for financial support under Indigenous 5000 Ph.D Fellowship program. J.S. thanks the Chemistry Department, University of Otago for support of his work. AF thanks the MINECO/AEI from Spain for a "Juan de la Cierva" contract. We thank the MINECO/AEI from Spain for financial support (project number CTQ2017-85821-R, FEDER funds). We are grateful to the CTI (UIB) for free allocation of computer time.

Supplementary Material

^{1}H and ^{13}C NMR spectra and crystal structures of compounds **5a–e**. CCDC: 1826226 (**5a**); 1826227 (**5b**); 1826228 (**5c**); 1826229 (**5d**); 1826230 (**5e**). For ESI and crystallographic data in CIF or other electronic format see online version of the manuscript.

References

1. H.-X. Dai, A. F. Stepan, M. S. Plummer, Y.-H. Zhang and J.-Q. You. *J. Am. Chem. Soc*., 2011, **133**, 7222–7228.

2. H. Göçer, A. Akıncıoğlu, N. Öztaskın, S. Göksu and I. Gülçin, *Arch. Pharm*., 2013, **346**, 783–792.

3. S. Mutahir, J. Jończyk, M. Bajda, I. U. Khan, M. A. Khan, N. Ullah, M. Ashraf, Qurat-ul-Ain, S. Riaz, S. Hussain and M. Yar, *Bioorg. Chem*., 2016, **64**, 13–20.

4. C. T. Supuran, *Nat. Rev. Drug Discov*., 2008, **7**, 168–181.

5. V. Alterio, A. Di Fiore, K. D'Ambrosio, C. T. Supuran and G. De Simone, *Chem. Rev*., 2012, **112**, 4421–4468.

6. G. De Simone, V. Alterio and C. T. Supuran, *Expert Opin. Drug Discov*., 2013, **8**, 793–810.

View Article Online
DOI: 10.1039/C8CE01917G

7. C. T. Supuran, *Bioorg. Med. Chem*., 2013, **21**, 1377–1378.

8. C. Capasso and C. T. Supuran, *J. Enzyme Inhib. Med. Chem*., 2014, **29**, 379–387.

9. C. Congiu, V. Onnis, A. Deplano, G. Balboni, N. Dedeoglu and C. T. Supuran, *Bioorg. Med. Chem. Lett*., 2015, **25**, 3850–3853.

10. P.-O. Markgrem, W. Schaal, M. Hamalainem, A. Karlen, A. Hallberg and B. Samuelsson, *J. Med. Chem*., 2002, **2**, 5430–5439.

11. B. R. Stranix, G. Sauvé, A. Bouzide, A. Coté, J. Y. Sévigny and V. Perron, *Bioorg. Med. Chem. Lett*., 2004, **14**, 3971–3974.

12. R. Crespo, M. G. De Bravo, P. A. Colinas and R. D. Bravo, *Bioorg. Med. Chem. Lett*., 2010, **20**, 6469–6474.

13. K. Takahashi, M. Ohta, Y. Shoji, M. Kassi, K. Kunishiro, T. Miilke, M. Kanada and H. Shirahase, *Chem. Pharma. Bull*., 2010, **58**, 1057–1065.

14. T. Tite, L. Tomas, T. Docsa, P. Gergely, J. Kovensky, D. Gueyrand and A. Wadouachi, *Tetrahedron. Lett*., 2012, **53**, 959–961.

15. W. Boufas, N. Dupont, M. Berredjem, K. Berrezag, I. Becheker, H. Berredjem and N.-E. Aouf, *J. Mol. Str*., 2014, **1074**, 180–185.

16. L. Gavernet and M. Dominguez-Cabrera, *Bioorg. Med. Chem*., 2007, **15**, 1556–1567.

17. A. R. Massah, H. Adibi, R. Khodarahmi, R. Abiri, M. B. Majnooni, S. Shahidi, B. Asadi, M. Mehrabi and M. A. Zolfigol, *Bioorg. Med. Chem*., 2008, **16**, 5465–5472.

18. M. Adib, E. Sheikhi and G. Sheikhi, *Tetrahedron Lett*., 2010, **51**, 5646–5648.

19. D. Liptrot, L. Alcaraz and B. Robberts, *Tetrahedron Lett*., 2010, **51**, 5341–5343.

20. S. Fu, X. Lian, T. Maa, W. Chen, M. Zheng and W. Zeng, *Tetrahedron. Lett*., 2010, **51**, 5834–5837.

View Article Online
DOI: 10.1039/C8CE01917G

21. F. Pacchiano, M. Aggarwal, B. S. Avvaru, A. H. Robbins, A. Scozzafava, R. McKenna and C. T. Supuran, *Chem. Commun*., 2010, **46**, 8371–8373.

22. F. Carta, M. Aggarwal, A. Maresca, A. Scozzafava, R. McKenna and C. T. Supuran, *Chem. Commun*., 2012, **48**, 1868–1870.

23. G. M. Brown, *Adv. Enzymol. Relat. Areas. Mol. Biol*., 1971, **35**, 35–77.

24. A. Casini, J. Antel, F. Abbate, A. Scozzafava, S. David, H. Waldeck, S. Schäfer and C. T. Supuran, *Bioorg. Med. Chem. Lett*., 2003, **13**, 841–845.

25. X.-C. Cheng, Q. Wang, H. Fang and W.-F. Xu, *Curr. Med. Chem*., 2008, **15**, 368–373.

26. T. H. Maren, *Physiol. Rev*., 1967, **47**, 595–781.

27. (a) J. W. Steed and J. L. Atwood, *Supramolecular Chemistry*, John Wiley & Sons, Ltd., UK, 2nd edn, 2009; (b) A Bauzá, S. K. Seth and A Frontera, Coord. Chem. Rev. 2019, 384, 107-125; (c)

28. (a) T. Shimizu, M. Masuda and H. Minamikawa, *Chem. Rev*., 2005, **105**, 1401-1444; (b) E. R. Kay, D. A. Leigh and F. Zerbetto, *Angew. Chem., Int. Ed*., 2007, **46**, 72-191; (c) J. D. Fox and S. J. Rowan, *Macromolecules*, 2009, **42**, 6823–6835.

29. G. R. Desiraju, *Chem. Commun*., 2005, 2995–3001.

30. G. R. Desiraju, *Acc. Chem. Res*., 2002, **35**, 565–573.

31. S. S. Kuduva, D. C. Craig, A. Nangia and G. R. Desiraju, *J. Am. Chem. Soc*., 1999, **121**, 1936–1944.

32. G. R. Desiraju and T. Steiner, *The Weak Hydrogen Bond in Structural Chemistry and Biology*, Oxford University Press, Oxford, U.K., 1999.

33. T. Steiner, *Chem. Commun*., 1997, 727–734.

View Article Online
DOI: 10.1039/C8CE01917G

34. C. R. Kaiser, K. C. Pais, M. V. N. de Souza, J. L. Wardell, S. M. S. V. Wardell and E. R. T. Tiekink, *CrystEngComm*, 2009, **11**, 1133–1140.

35. (a) L.-F. Ma, L.-Y. Wang, J.-L. Hu, Y.-Y. Wang, S. R. Batten and J.-G. Wang, *CrystEngComm*, 2009, **11**, 777–783; (b) R. Bag, Y Sikdar, S. Sahu, D. K. Maiti, A. Frontera, A. Bauzá, M. G. B. Drew and S. Goswani, *Dalton Trans*., 2018, **47**, 17077-17085; (c) B. Naskar, A. Bauzá, A. Frontera, D. K. Maiti, C. D. Mukhopadhyay, S. Goswami, *Dalton Trans*., 2018, **47**, 15907-15916; (d) K. Ghosh, K. Harms, A. Bauzá, A. Frontera, S. Chattopadhyay, *CrystEngComm* 2018, **20**, 7281-7292; (e) S. Saha, N. Biswas, A. Sasmal, C. J. Gómez-García, E Garribba, A Bauza, A. Frontera, G. Pilet, G. M. Rosair, S. Mitra, C. R. Choudhury, *Dalton Trans*., 2018, **47**, 16102-16118

36. (a) H. Zhou, L. Chen, R. Chen, Z.-H. Peng, Y. Song, Z.-Q. Pan, Q.-M. Huang, X.-L. Hu and Z.-W. Bai, *CrystEngComm*, 2009, **11**, 671–679; (b) S. Dutta, S. Jana, P. Mahapatra, A. Bauzá, A. Frontera and A. Ghosh, *CrystEngComm*, 2018, **20**, 6490–6501; (c) A. Castiñeiras, I. García-Santos, J. M. González-Pérez, A. Bauzá, J. K. Zaręba, J. Niclós-Gutiérrez, R. Torres, E. Vílchez and A. Frontera, *Cryst. Growth Des*., 2018, **18**, 6786–6800; (d) M. N. Piña, P. Rodríguez, M. S. Gutiérrez, D. Quiñonero, J. Morey and A. Frontera, *Chem. Eur. J*. 2018, **24**, 12820-12826; (e) T. Maity, H. Mandal, A. Bauza, B. C. Samanta, A. Frontera and S. K. Seth, *New J. Chem*., 2018, **42**, 10202–10213; (f) G. Mahmoudi, S. K. Seth, A. Bauza, F. I. Zubkov, A. V. Gurbanov, J. White, V. Stilinovic, T. Doert and A. Frontera *CrystEngComm*, 2018, **20**, 2812–2821.

37. (a) Y. R. Zhong, M. L. Cao, H. J. Mo and B. H. Ye, *Cryst. Growth Des*., 2008, **8**, 2282–2290; (b) A. Gogoi, S. M. Nashre-ul-Islam, A. Frontera and M. K. Bhattacharyya, *Inorg. Chim. Acta*, 2019, **484**, 133-141

View Article Online
DOI: 10.1039/C8CE01917G

38. (a) S. Takahashi, T. Jukurogi, T. Katagiri and K. Uneyama, *CrystEngComm*, 2006, **8**, 320–326; (b) R. Barbas, R. Prohens, A. Bauzá, A. Franconetti, A. Frontera, *Chem. Commun*., 2019, **55**, 115-118; (c) G. Mahmoudi, A. A. Khandar, F. A. Afkhami, B. Miroslaw, A. V. Gurbanov, F. I. Zubkov, A. Kennedy, A. Franconetti and A. Frontera, *CrystEngComm*, 2019, **21**, 108–117; (d) B. Ramezanpour, M. Mirzaei, V. Jodaian, M. N. Shahrak, A. Frontera, E. Molins, *Inorg. Chim. Acta*, 2019, **484**, 264–275.

39. (a) A. N. Sokolov, T. Friscic, S. Blais, J. A. Ripmeester and L. R. MacGillivray, *Cryst. Growth Des*., 2006, **6**, 2427–2428; (b) S. M. Nashre-ul-Islam, D. Dutta, A. Frontera, M. K. Bhattacharyya, *Inorg. Chim. Acta*, 2019, **487**, 424–432; (c) D. Quiñonero and A. Frontera, *Inorganics*, 2019, **7**, 9; (d) M. Kumar, H. N. Sheikh, A. Franconetti, J. K. Zaręba and A. Frontera, *New J. Chem*. 2019, **43**, 2179–2195.

40. S. K. Panigrahi, *Amino Acids*, 2008, **34**, 617–633.

41. G. Toth, S. G. Bowers, A. P. Truong and G. Probst, *Curr. Pharm. Des*., 2007, **13**, 3476–3493.

42. S. Sarkhel and G. R. Desiraju, *Proteins: Struct., Funct., Genet*., 2004, **54**, 247–259.

43. E. Arbely and I. T. Arkin, *J. Am. Chem. Soc*., 2004, **126**, 5362–5363.

44. B. K. Ho and P. M. Curmi, *J. Mol. Biol*., 2002, **317**, 291–308.

45. O. B. Berryman, V. S. Bryantsev, D. P. Stay, D. W. Johnson and B. P. Hay, *J. Am. Chem. Soc*., 2007, **129**, 48–58.

46. (a) Y. Bai, B.-G. Zhang, C.-Y. Duan, D.-B. Dang and Q.-J. Meng, *New J. Chem*., 2006, **30**, 266–271; (b) S. Khan, S. Roy, K. Harms, A. Bauzá, A. Frontera and S. Chattopadhyay, *Inorg. Chim. Acta*, 2019, **487**, 465-472.

47. I. Hisaki, S.-I. Sasaki, K. Hirose and Y. Tobe, *Eur. J. Org. Chem*., 2007, 607–615.

View Article Online
DOI: 10.1039/C8CE01917G

48. K.-J. Chang, D. Moon, M. S. Lah and K.-S. Jeong, *Angew. Chem., Int. Ed*., 2005, **44**, 7926–7929.

49. (a) T. Hajiashrafi, R. Zekriazadeh, K. J. Flanagan, F. Kia, A. Bauzá, A. Frontera and M. O. Senge, Acta Cryst. 2019, C75, 178-188; (b) U. Saha, D. Dutta, H. Nath, A. Franconetti, A. Frontera and M.K. Bhattacharyya, *Inorg. Chim. Acta*, 2019, **488**, 159-169; (c) F. A. Afkhami, G. Mahmoudi, A. A. Khandar, A. Franconetti, E. Zangrando, N. Qureshi, J. Lipkowski, A. V. Gurbanov, A. Frontera, *Eur. J. Inorg. Chem*. 2019, 262-270. (d) H. Ihm, S. Yun, H. G. Kim, J. K. Kim and K. S. Kim, *Org. Lett*., 2002, **4**, 2897.

50. J. S. González-González, F. J. Martínez-Martínez, A. L. P. Campos, M. de Jesus Rosales-Hoz, E. V. García-Báez and I. I. Padilla-Martínez, *CrystEngComm*, 2011, **13**, 4748-4761.

51. (a) R. Carrillo, M. López-Rodríguez, V. S. Martin and T. Martín, *Angew. Chem., Int. Ed*., 2009, **48**, 7803-7808; (b) Y. Kobayashi, T. Kurasawa, K. Kinbara and K. Saigo, *J. Org. Chem*., 2004, **69**, 7436-7441; (c) Y. Ryan, P. W. Peterson, C. M. Hadad and J. D. Badjic, *Chem. Commun*., 2014, **50**, 9086-9089; (d) P. Sozzani, A. Comotti, S. Braco and R. Simonutti, *Chem. Commun*., 2004, 768; (e) H. Brunner, T. Tsuno and M. Bodensteiner, *Organometallics*, 2014, **33**, 2257-2265; (f) E. C. Constable, K. Harris, C. E. Housecroft, M. Neuburger and J. A. Zampese, *CrystEngComm*, 2010, **12**, 2949-2961; (g) C. D. Scala, H. Chahinian, N. Yahi, N. Garmy and J. Fantini, *Biochemistry*, 2014, **53**, 4489-4502; (h) A. K. Pandey, K. M. Thomas, C. R. Forbes and N. J. Zondlo, *Biochemistry*, 2014, **53**, 5307-5314; (i) M. Kufmann, M. Gisler and C. J. Leumann, *Angew. Chem., Int. Ed*., 2009, **48**, 3810-3813; (j) S. M. Butterfield, M. M. Sweeney and M. L. Waters, *J. Org. Chem*., 2005, **70**, 1105-1114; (k) M. Kumar and P. V. Balaji, *J. Mol. Model*., 2014, **20**, 2136; (l) M. Brandl, M. S. Weiss, A. Jabs, J. Sühnel and R. Hilgenfeld, *J. Mol. Biol*., 2001, **307**, 357-377.

View Article Online
DOI: 10.1039/C8CE01917G

52. (a) M. Shafique, S. Hameed, M. M. Naseer and N. A. Al-Masoudi, *Mol. Divers.*, 2018, **22**, 957-968; (b) C. S. Shultz, S. D. Dreher, N. Ikemoto, J. M. Williams, E. J. J. Grabowski, S. W. Krska, Y. Sun, P. G. Dormer and L. DiMichele, *Org. Lett*., 2005, **7**(16), 3405–3408.

53. I. Khan, S. Ali, S. Hameed, N. H. Rama, M. T. Hussain, A. Wadood, R. Uddin, Z. Ul-Haq, A. Khan, S. Ali and M. I. Choudhary, *Eur. J. Med. Chem*., 2010, **45**, 5200–5207.

54. I. Khan, M. Hanif, M. T. Hussain, A. A. Khan, M. A. S. Aslam, N. H. Rama and J. Iqbal, *Aust. J. Chem.*, 2012, **65**, 1413–1419.

55. (a) N. Halland and K. A. Jørgensen, *J. Chem. Soc., Perkin Trans*., 2001, **1**, 1290–1295; (b) G. Reischl, M. El-Mobayed, R. Beisswenger, K. Regier, C. Maichle-Moessmer and A. Rieker, Z. *Naturforsch. B Chem. Sci*., 1998, **53**, 765–773; (c) Q.-H. Zheng, G. D. Hutchins, B. H. Mock and W. L. Winkle, *J. Labelled Comp. Radiopharm*., 2001, **44**, S104–S106; (d) M. Zareef, R. Iqbal, N. A. Al-Masoudi, J. H. Zaidi, M. Arfan and S. A. Shahzad, *Phosphorus Sulfur Silicon Relat. Elem*., 2007, **182**, 281–298.

56. *APEX2*, *SAINT* and *SADABS*, Bruker AXS Inc., Madison, Wisconsin, USA, 2007.

57. G. M. Sheldrick, *Acta Cryst.,* 2008, A**64**, 112-122.

58. G. M. Sheldrick, *Acta Cryst.,* 2015, C**71**, 3-8.

59. C. F. Macrae, I. J. Bruno, J. A. Chisholm, P. R. Edgington, P. McCabe, E. Pidcock, L. Rodriguez-Monge, R. Taylor, J. van de Streek and P. A. Wood, *J. Appl. Cryst.*, 2008, **41**, 466-470.

60. A. L. Spek, *Acta Cryst*., 2009, D**65**, 148-155.

61. L. J. Farrugia, *J. Appl. Cryst.*, 2012, **45**, 849-854.

62. Gaussian 09, Revision C.01 M. J. Frisch, G. W. Trucks, H. B. Schlegel, G. E. Scuseria, M. A. Robb, J. R. Cheeseman, G. Scalmani, V. Barone, B. Mennucci, G. A. Petersson, H. Nakatsuji,

View Article Online
DOI: 10.1039/C8CE01917G

M. Caricato, X. Li, H. P. Hratchian, A. F. Izmaylov, J. Bloino, G. Zheng, J. L. Sonnenberg, M. Hada, M. Ehara, K. Toyota, R. Fukuda, J. Hasegawa, M. Ishida, T. Nakajima, Y. Honda, O. Kitao, H. Nakai, T. Vreven, J. A. Montgomery, Jr., J. E. Peralta, F. Ogliaro, M. Bearpark, J. J. Heyd, E. Brothers, K. N. Kudin, V. N. Staroverov, R. Kobayashi, J. Normand, K. Raghavachari, A. Rendell, J. C. Burant, S. S. Iyengar, J. Tomasi, M. Cossi, N. Rega, J. M. Millam, M. Klene, J. E. Knox, J. B. Cross, V. Bakken, C. Adamo, J. Jaramillo, R. Gomperts, R. E. Stratmann, O. Yazyev, A. J. Austin, R. Cammi, C. Pomelli, J. W. Ochterski, R. L. Martin, K. Morokuma, V. G. Zakrzewski, G. A. Voth, P. Salvador, J. J. Dannenberg, S. Dapprich, A. D. Daniels, Ö. Farkas, J. B. Foresman, J. V. Ortiz, J. Cioslowski and D. J. Fox, Gaussian 09 (Gaussian, Inc., Wallingford CT, 2009).

63. AIMAll (Version 17.01.25), T. A. Keith, Gristmill Software, Overland Park KS, USA, 2013.

64. E. R. Johnson, S. Keinan, P. Mori-Sanchez, J. Contreras-Garcia, A. J. Cohen and W. Yang, *J. Am. Chem. Soc*., 2010, **132**, 6498-6506.

65. T. Syed, T. Akhtar, N. A. Al-Masoudi, P. G. Jones and S. Hameed, *J. Enzyme Inhib. Med. Chem.*, 2011, **26**, 668–680.

66. H. Purandara, S. Foro and B. T. Gowda, *Acta Cryst*., 2015, **E71**, 730–733.

67. H. Purandara, S. Foro and B. T. Gowda, *Acta Cryst*., 2015, **E71**, 602–605.

68. R. F. W. Bader, *J. Phys. Chem. A*, 1998, **102**, 7314–7323.

69. R. F. W. Bader, *Chem. Rev*., 1991, **91**, 893–928.

70. J. Contreras-García, E. R. Johnson, S. Keinan, R. Chaudret, J.-P. Piquemal, D. N. Beratan and W. Yang, *J. Chem. Theory Comput*., 2011, **7**, 625–632

View Article Online
DOI: 10.1039/C8CE01917G

Five new hydrazinyl-sulfonamides with pendant linear and branched alkyl chains are synthesized and X-ray characterized. The U-shaped conformation observed in the solid state of all compounds has been analyzed using DFT calculations.